- Hydroxycinnamoyl-coenzyme A:tetrahydroxyhexanedioate
 hydroxycinnamoyl transferase (HHHT) from *Phaseolus vulgaris* L.: Phylogeny, expression pattern, kinetic
 parameters, and active site analysis
 Amanda Fanelli^{1,2}, Christina Stonoha-Arther¹, and Michael L. Sullivan¹
 ¹US Dairy Forage Research Center, Agricultural Research Service, United States Department of
- Amanda Fanelli^{1,2}, Christina Stonoha-Arther¹, and Michael L. Sullivar
 ¹US Dairy Forage Research Center, Agricultural Research Service, Un
 Agriculture, Madison, WI, USA
 ²Oak Ridge Institute of Science and Education, Oak Ridge, TN, USA
 Corresponding Author
 Amanda Fanelli
 USDFRC, 1925 Linden Drive, Madison, WI 53706, USA

Email address: amanda.fanelli@usda.gov

16 17 18

Abstract

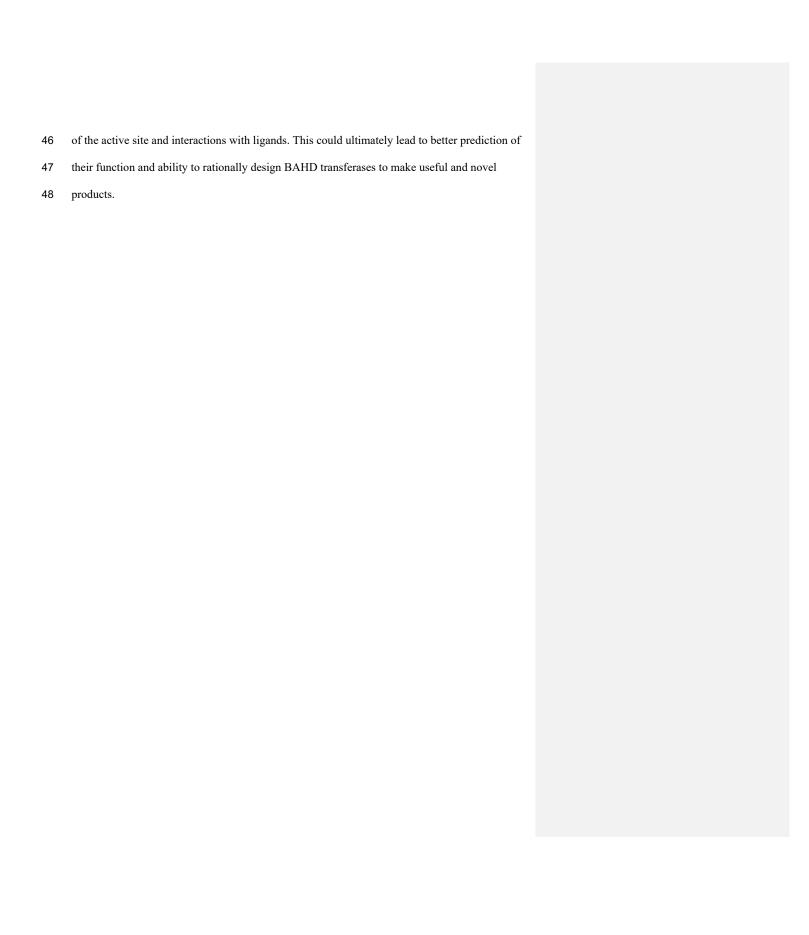
20 21

19

22 BAHD acyl-Coenzyme A (CoA) transferases comprise a large family of enzymes in plants which transfer an acyl group from a CoA thioester to hydroxyl or amine groups to form esters or 23 24 amides, respectively. Clade Vb of this family primarily utilizes hydroxycinnamoyl-CoA as the 25 acyl donor. These enzymes are involved in biosynthesis of diverse specialized metabolites with functions such as structure (e.g. lignin formation) and biotic/abiotic stress mitigation. The 26 27 diversity of these enzymes has arisen from both divergent and convergent evolution, making it 28 difficult to predict substrate specificity or enzyme function based on homology, and relatively 29 few BAHD transferases have been characterized biochemically with respect to substrate specificity. We previously identified a hydroxycinnamoyl-CoA:tetrahydroxyhexanedioate 30 31 hydroxycinnamoyl transferase (HHHT) from common bean capable of transferring 32 hydroxycinnamic acids to mucic or saccharic acid to form the corresponding esters. Here, to 33 better understand the structure/function relationships of this enzyme, we have further 34 characterized it with respect to expression pattern, kinetic parameters, and predicted three-35 dimensional (3-D) structure and active site interactions with acceptor substrates. HHHT was expressed predominantly in leaves and to a lesser extent flowers and shoots. $K_{\rm M}$ values did not 36 37 vary greatly among donor or acceptor substrates (generally less than two-fold), while kcat values 38 were consistently higher for saccharic acid as substrate compared to mucic acid, leading to 39 higher catalytic efficiency (as $k_{\text{cat}}/K_{\text{M}}$) for saccharic acid. Both acceptors had similar binding 40 poses when docked into the active site, and the proximity of multiple hydroxyl groups to the catalytic His-150, especially for saccharic acid, might provide some insights into 41 regiospecificity. These findings provide a foundation for better understanding how the 3-D 42 43 structure of BAHD transferases relates to their substrate specificity, as we explore the chemistry

Deleted: vales

Deleted: among



Introduction

50 51 52

53 54

55

56

57

58

59

60

61

62

63

64

65

66

67

68

69

70

49

Acylation is an important step in the synthesis of several plant metabolites. Many of these processes involve enzymes belonging to the BAHD acyltransferase family, which catalyze the transfer of an acyl group from a coenzyme A (CoA) thioester to alcohol or amine groups, producing esters or amides, respectively (Bontpart et al. 2015). BAHD acyltransferases Field Code Changed participate in the synthesis of anthocyanins, flavonoids, cell wall components, and other specialized metabolites (Moghe et al. 2023). Phylogenetic analyses have divided this family into Field Code Changed eight clades (Tuominen, Johnson, and Tsai 2011) named Ia, Ib, II, IIIa, IIIb, IV, Va, and Vb. Field Code Changed There is evidence of both divergent and convergent evolution in the BAHD family. Consequently, similarity of amino acid sequence does not always indicate similar substrate specificities. There are enzymes that share high sequence similarity but use different substrates (Kruse et al. 2022; Sullivan and Knollenberg 2021), and also enzymes with low sequence Field Code Changed similarity that have similar catalytic roles (Fu et al. 2022). Therefore, it is difficult to use Field Code Changed homology to predict function (Luo et al. 2007). Furthermore, a limited number of BAHD Field Code Changed enzymes have had their three-dimensional (3-D) structure elucidated or were characterized with respect to kinetic parameters and substrate specificity, which also contributes to the difficulty of

71 72

73

In clade Vb of BAHD acyltransferases, characterized enzymes catalyze reactions in which aromatic acids, predominately hydroxycinnamates, are the donated acyl group. The Vb enzymes

predicting the catalytic function based on the amino acid sequence. Nevertheless, the recent

improvement of algorithms for 3-D protein 3-D structure prediction and molecular docking is

promising to allow a better understanding of the relationship between structure and substrate

specificity in the BAHD family (Jisna and Jayaraj 2021; Fanelli and Sullivan 2022).

Field Code Changed

74	have roles in the synthesis of compounds related to plant development and defense, such as	
75	lignin precursors, phaselic acid, hydroxycinnamoyl spermidines, and phytoalexins. Therefore,	
76	this clade is an attractive target for many biotechnological and metabolic engineering	
77	applications (Yang et al. 2004; Grienenberger et al. 2009; Hoffmann et al. 2005; Sullivan 2009).	Field Code Changed
78		
79	In red clover (Trifolium pratense L.), we have shown that two clade Vb enzymes, HMT and	
80	HDT, are responsible for the accumulation of the caffeoyl derivatives phaselic acid [2-O-	
81	caffeoyl-L-malic acid] and clovamide [N-caffeoyl-L-3,4-dihydroxyphenylalanine] [Sullivan and	Field Code Changed
82	Zarnowski 2011; Sullivan and Knollenberg 2021; Sullivan 2009). The oxidation of these	
83	compounds by polyphenol oxidases (PPO) may have a role in the defense against insect	
84	herbivores and pathogens (Constabel and Barbehenn 2008). This process also has applications in	Field Code Changed
85	improving forages for animal feed, as the oxidation of these o -diphenols by PPO reduces post-	
86	harvest protein degradation after ensiling (Sullivan and Hatfield 2006). The PPO/o-diphenol	Field Code Changed
87	system could be transferred to other forages, such as alfalfa, that do not naturally possess it to	
88	mitigate protein losses when ensiled. However, we have demonstrated that red clover HMT has a	
89	greater than five-fold preference ($V_{ m max}/K_{ m M}$) for p -coumaroyl- or feruloyl-CoA as an acyl donor	
90	over caffeoyl-CoA (Sullivan and Zarnowski 2011), and overexpression of red clover HMT in	Field Code Changed
91	alfalfa ($Medicago\ sativa\ L$.) results in the accumulation of mostly p -coumaroyl- and feruloyl-	
92	malate, not phaselic acid (Sullivan, Green, and Verdonk 2021). These p-coumaroyl and feruloyl	Field Code Changed
93	derivatives are ineffective at preventing protein degradation (Sullivan and Zeller 2013). In the	Field Code Changed
94	search for an HMT from <i>Phaseoulus vulgaris</i> L. (common bean, hereafter referred to as bean)	
95	that might have a stronger preference for caffeoyl-CoA, we identified a hydroxycinnamoyl-	
96	CoA:tetrahydroxyhexanedioic acid hydroxycinnamoyl transferase (HHHT), which transfers	

hydroxycinnamates to mucic and saccharic acid acceptors to form the corresponding esters (Fig. 97 98 1) (Sullivan 2017). Field Code Changed 99 100 Although it has been suggested that these compounds may also be involved in plant defense, 101 little is known about the role of HHHT in beans. Furthermore, the kinetic parameters for this Deleted: bean 102 enzyme have not been measured, and it is unknown whether HHHT prefers a specific acyl donor 103 or acceptor. Along with kinetic data, elucidating the enzyme's 3-D structure and active site may 104 give information about how enzyme structure influences substrate preference, which could be 105 used for the rational design of BAHD enzymes. In this study, we sought to investigate the 106 evolutionary relationship of bean HHHT with other enzymes in clade Vb and gain insights about 107 its function, enzyme kinetics, structure, and active site. 108 109 **Materials and Methods** 110 111 112 Annotation of BAHD transferases and phylogenetic analysis. 113 114 To annotate putative BAHD acyltransferases in *Phaseolus vulgaris*, *Trifolium pratense*, 115 Medicago truncatula Gaetrn., Arabidopsis thaliana (L.) Heynh., Brachypodium distachion (L.) 116 P.Beauv. and Panicum Hallii Vasey, the hmmsearch algorithm was used on the EMBL-EBI 117 website (https://www.ebi.ac.uk/Tools/hmmer/search/hmmsearch) (Potter et al. 2018). An Field Code Changed Field Code Changed 118 accession search was performed using PF02458 at PFAM (transferase) profile against the 119 Ensembl proteomes database, restricting to the species mentioned. From all sequences returned, 120 only those with an e-value $< 10^{-5}$ were considered as true positive results. Isoforms (that had 121 duplicate names in the database) were identified using a Python script, and only one sequence

123	per coding gene was kept for analysis. To annotate clade Vb from BAHD acyltransferases, a	
124	phylogenetic analysis was performed with the set of transferases identified by hmmsearch and a	
125	set of 69 characterized BAHD proteins (Tuominen, Johnson, and Tsai 2011), which were	Field Code Changed
126	downloaded from NCBI. The two sets were compared to remove any duplicates. These	
127	sequences were aligned using MUSCLE5 in seaview5 software (Gouy et al. 2021). The	Field Code Changed
128	alignment was inspected for the presence of the active site HXXXD motif. Sequences that had	
129	this region conserved were kept for analysis. We also included sequences that had a residue	
130	other than H in the first position of the motif, as a biochemically characterized BAHD has this	
131	His replaced by Ser (Walker, Long, and Croteau 2002). To place the root in the phylogenetic	Formatted: English (US)
132	tree, a set of three transferase sequences from fungi (RHIMIDRAFT_244343 from Rhizopus	
133	microspores, DM01DRAFT_1381931 from Hesseltinella vesiculosa, and	
134	BCR42DRAFT_237763 from Absidia repens) were annotated using hmmsearch as above and	Formatted: English (US)
135	included in the analysis as an outgroup. After obtaining this final set, all sequences were aligned	
136	using MUSCLE5 in seaview5 software. The alignment was manually edited, and a maximum	
137	likelihood phylogeny was built using the IQ-Tree webserver (http://igtree.cibiv.univie.ac.at/)	Field Code Changed
138	(Trifinopoulos et al. 2016). Branch support was obtained using SH-aLRT. The best-fit model,	Field Code Changed
139	chosen by ModelFinder (Kalyaanamoorthy et al. 2017) using BIC criteria, was VT + F + G4.	Field Code Changed
140	The tree was visualized using iTOL (Letunic and Bork 2021). After identifying clade Vb in the	Field Code Changed
141	BAHD phylogeny, another phylogenetic tree was inferred only for the members of this clade,	
142	with four sequences from other clades used as an outgroup to root the tree, plus a set recently	
143	characterized (Supplemental Table S1). The parameters were as before, and the best-fit model	
144	chosen was $JTT + I + G4$. The final tree was visualized with iTOL and edited using Figma.	
145		

146	Gene expression and cis-element promoter analysis.		
147			
148	We analyzed RNA-seq data from O'Rourke et al. 2014 available at	F	ield Code Changed
149	https://www.zhaolab.org/PvGEA/, and from Ayyappan et al. 2015. The work from O'Rourke et	F	ield Code Changed
150	al. provided RNA-seq data for the <i>Phaseolus vulgaris</i> cultivar 'Negro Jamapa'. Samples	D	eleted: Phaselous
1 151	consisted of seven tissues at specific developmental stages, and three nitrogen treatments that		
152	consisted of inoculating nodules with the effective nitrogen _z fixing strain <i>Rhizobium tropici</i>	D	eleted:
153	CIAT899, or with the ineffective strain Rhizobium giardini 6917, or providing fertilizer	D	eleted: Giardini
154	containing adequate levels of NO3° for growth. The work from Ayyappan et al. analyzed RNA-		
155	seq data for leaves of the bean cultivar 'Sierra' inoculated with the fungal rust Uromyces		
156	appendiculatus. Time points for sample collection were 0, 12, and 84 h after inoculation. The	D	eleted: hours
157	meta-analysis and visualization in our work here were performed using R. The search for cis-		
158	elements in the promoter region of the <i>Pvhhht</i> gene was conducted by using the 600 bp region		
159	upstream as a query in the newPLACE database		
160	(https://www.dna.affrc.go.jp/PLACE/?action=newplace) (Higo et al. 1999).	F	ield Code Changed
161		F	ield Code Changed
101			
162	Expression of <i>Phaseolus vulgaris</i> HHHT in <i>Escherichia coli</i> and purification of the his-		
163	tagged protein.		
164			
165	DNA encoding HHHT was synthesized by GenScript (Piscataway, NJ, USA) based on the		
166	predicted amino acid sequence (Genbank AOX15526.1) of the previously characterized cDNA		
167	(Genbank KX443573) with codon optimization for E. coli using the supplier's algorithm and	(D	alatada NJ- I
168	specifying <u>Ndel</u> and <u>Xhol</u> be absent from the open reading frame. The sequence CAT was added	\sim	eleted: Nde I eleted: Xho I
I			

175	to the 5' end to create an <u>Ndel</u> site, and a TAA stop codon and <u>Xhol</u> site were added to the 3'		eleted: Nde I
176	end. The synthesized DNA (Genbank ON240067) was cloned as an <u>NdeI - XhoI</u> fragment	\succ	prmatted: Font: Italic eleted: Nde I - Xho I
		De	reteu: Nue 1 - Alio 1
177	between those restriction sites of pET28a(+) (MilliporeSigma, Burlington, MA, USA). The		
178	resulting construct fuses a <u>6xHis</u> -tag to the N-terminus of HHHT.	De	eleted: 6xhis
l 179			
180	The pET28-based construct was transformed into Rosetta 2 (DE3) pLysS competent cells		
181	(MilliporeSigma). Transformed cells were grown and induced, and a lysate of the cells was made		
182	essentially as described in the pET System Manual (available at http://emdmillipore.com as		
183	TB055). A 1 L culture in LB medium with 50 $\mu g/mL$ of kanamycin and 34 $\mu g/mL$		
184	chloramphenicol was grown with shaking at 37 $^{\circ}\text{C}$ to an $OD_{600\text{nm}}$ of 0.54, induced with isopropyl		
185	β-D-1-thiogalactopyranoside (IPTG) added to 1 mM, then grown an additional 20 h at 18 °C.		
186	The cells were harvested by centrifugation, resuspended in 20 mL Bugbuster reagent		
187	(MilliporeSigma) to which <u>10 μL</u> benzonase nuclease and 200 μL protease inhibitor cocktail	De	eleted: 10µL
188	were added (70746 and P8849, respectively, MilliporeSigma), and incubated at room		
189	temperature for 20 min. Insoluble material was removed by centrifugation at 17,000 x g for 10	Fo	ormatted: Font: Italic
190	min at 4 °C. To the 20 mL of cleared lysate, 80 mL of 1.25 X binding buffer (1 X is 20 mM		
191	sodium phosphate, pH 7.5, 500 mM NaCl, 20 mM imidazole) was added. The non-proteinaceous		
192	precipitate that formed upon binding buffer addition was removed by centrifugation at 30,000 x		
193	g for 10 min at 4 °C, and the clarified sample was added to 1 mL Ni-Sepharose 6 Fast Flow	Fo	ormatted: Font: Italic
194	(Catalog 17-5318-01, GE Healthcare BioScience AB, Uppsala, Sweden) that had been washed		
195	and pre-equilibrated with binding buffer. Tagged protein was allowed to bind to the Ni-		
196	Sepharose by incubating at room temperature on a nutator for 80 min. The Ni-Sepahrose was		
197	transferred to a small column, washed five times with 1 mL of binding buffer, and the protein		
•			

202	was eluted with 3 mL of 250 mM imidazole in 20 mM sodium phosphate, pH 7.5, 500 mM	
203	NaCl. The eluate was dialyzed overnight against 500 mL 20 mM sodium phosphate, pH 7.5, 500	
204	mM NaCl at 4 °C. The sample was further concentrated, and the buffer was exchanged to 100	
205	mM sodium phosphate, pH 7.5 using an Amicon Ultra-15 concentrator (MilliporeSigma) with a	
206	10,000 molecular weight cutoff. Aliquots were made, flash frozen in liquid nitrogen, and stored	Deleted:
207	at -60 °C until needed for analyses. The protein concentration of the purified protein was	Deleted: Protein
1 208	estimated by comparison to known amounts of bovine serum albumin on SDS-PAGE gels.	
209		
210	In addition to the wild-type HHHT, four putative active site mutant gene constructs were	Deleted:
211	synthesized (T35A, H150A, W386A, and R414A) by replacing the corresponding codons of the	Formatted: English (US) Formatted: English (US)
212	codon-optimized version of the gene with GCG. These were transformed and expressed in E.	
213	coli, and protein was purified as described above for the wild type.	
214		
215	Determination of HHHT kinetic parameters.	
216		
217	Kinetic parameters for HHHT were determined by measuring initial reaction rates by release of	Formatted: English (US)
218	free CoA in near-real time using DTNB (5,5'-dithio-bis- [2-nitrobenzoic acid]) and spectroscopy	
219	as detailed elsewhere (Sullivan and Bonawitz, 2018; Sullivan 2023). Measurements were made	
220	in a temperature-controlled spectrophotometer at 25 °C. Reactions (1 mL final volume) were	
221	carried out in 100 mM sodium phosphate, 1 mM EDTA, 0.2 mM DTNB. Acceptor substrates	Deleted:
222	were prepared as 50 mM stock solutions of the dipotassium salt by adding two equivalents of	Formatted: English (US)
223	KOH to mucic acid (M89617, MilliporeSigma) and one equivalent of KOH to the saccharic acid	
	11011 to made acid (1105017, 111111poreosignia) and one equivalent of front to the successive acid	

228	monopotassium salt (S4140, MilliporeSigma), to enhance solubility. The substrate and enzyme		Deleted:
			Deleted: Substrate
229	amounts used are detailed in Table 1.	1	Formatted: English (US)
220		1	Formatted: English (US)
230			
231	All kinetic data analyses were carried out using GraphPad Prism version 8 for Mac OS X		
232	(GraphPad Software, La Jolla, CA, USA). Each analysis (i.e., series of substrate concentrations)		
233	was carried out in duplicate with freshly prepared substrate and enzyme dilutions. Data were		
234	analyzed by non-linear regression of the replicated data. All donor/acceptor substrate		
235	combinations were fit with the Michaelis-Menten enzyme kinetics model. Kinetic parameters are		
236	reported \pm standard error (SE) as determined from the non-linear regression.		
237			
238	Structure prediction and molecular docking.		
239			
240	A pdb file (AF-V7BKA6-F1-v4) with the coordinates of the predicted three-dimensional		Formatted: English (US)
241	$structure\ of\ PvHHHT\ was\ downloaded\ from\ the\ AlphaFold\ website\ (https://alphafold.ebi.ac.uk/).$		
242	The quality of the model was evaluated using MolProbity (Williams et al. 2018). The molecules		Formatted: English (US)
			Formatted: English (US)
243	of the two acyl acceptor ligands, saccharic acid and mucic acid, were rendered using Avogadro		Field Code Changed
244	(v 1.2.0). The protonation state used was for a pH of 7.4. A conformer search was performed to		
245	find the minimum energy conformation, as described (Fanelli and Sullivan 2022). The final		Formatted: English (US)
	5,	<u></u>	Formatted: English (US)
246	coordinates were saved in <i>mol2</i> files. AutoDockVina (v 1.2.5) (Eberhardt et al. 2021) was used		Formatted: English (US)
			Field Code Changed
247	to perform the molecular docking of the ligands into the enzyme. To generate the <i>pdbqt</i> files	1/	Formatted: English (US)
248	required by Vina, the Python Meeko package was used for the ligands, using the	\	Field Code Changed
249	mk_prepare_ligand.py script. For the protein, the ADFR software suite (Ravindranath et al.		Formatted: English (US)
250	2015)		Field Code Changed
250	2015) was used. For the docking, the coordinates of the center were set to be the center of mass		Formatted: English (US)
1			

253	of the HXXXD active site motif, as described (Fanelli and Sullivan 2022), the search space was	***************************************	Formatted: English (US)
254	20 x 20 x 20 Å, and the exhaustiveness was set to 32, therefore allowing the bonds to rotate. The	***************************************	Field Code Changed
255	results were visualized using Pymol. To perform docking for the acyl donors (p-coumaroyl,		
256	caffeoyl-, and feruloyl-CoA), we used only a portion of the molecule (N-acetyl-S-		
257	hydroxycinnamoyl-cysteamine), since the CoA is too large to be handled by the Vina algorithm.		
258	The molecules were rendered, and the docking was performed as described for the acceptors.		Deleted: accepetors
			Formatted: English (US)
259			Formatted: English (US)
260	Results and Discussion		
261			
262	Phylogenetic analysis of clade Vb of BAHD acyltransferases.		
263			
264	To explore the evolution of BAHD acyltransferases in bean, particularly clade Vb, relative to		
265	other species, we identified BAHD sequences in the proteomes of four dicots (bean, red clover,		
266	Medicago truncatula, Arabidopsis) and two grasses (Panicum hallii and Brachypodium	***************************************	Deleted: arabidopsis
267	distachion), and analyzed their phylogenetic relationship to a set of biochemically characterized		
268	BAHD enzymes (Table 2). The genomes analyzed here encode a large number of BAHD		
269	acyltransferases, consistent with the many roles of this family having several distinct roles in		
270	plants, such as the synthesis of anthocyanins/flavonoids (clade Ia), epicuticular waxes (clade II),		
271	volatile esters (clade Va), acylation of oligosaccharide sugars, alkaloids, and terpenes (clade		
272	IIIa), aliphatic amine acylation (clade IV), among other functions (Moghe et al. 2023). As		Formatted: English (US)
273	observed in other studies, the distribution among clades varies depending on the species, and		
274	clade IV seems to be predominantly present in grasses, whereas clade IIIa seems specific to		
275	dicots (Tuominen, Johnson, and Tsai 2011; Bartley et al. 2013).		Field Code Changed

278 279 We then performed a more detailed analysis of clade Vb (Fig. 2). In this clade, we identified two 280 major subclades. One contains mostly HCT/HQT sequences, which are involved in the synthesis 281 of monolignols and chlorogenic acid, but also includes AsHHT from oats (Yang et al. 2004) and Field Code Changed 282 DcHCBT from Dianthus caryophyllus (Yang et al. 1997), which transfer aromatic groups, such Field Code Changed 283 as benzoyl and hydroxycinnamoyl, to anthranilates, producing amides that are precursors of 284 phytoalexins. It also contains the recently identified EpHMT from Echinacea purpurea, which 285 transfers hydroxycinnamates to malic acid, producing phaselic acid. The other subclade is 286 expanded in dicots, with no representative of the grasses Panicum halli and Brachypodium 287 distaction, which suggests that these enzymes may have roles specific to dicots. This subclade 288 further subdivides into two. One contains Arabidopsis thaliana AtSHT (spermidine Deleted: Arabidosis 289 hydroxycinnamoyl transferases (SHT) identified in dicots such as Arabidopsis thaliana, 290 Helianthus annus and Malus domestica). These characterized enzymes are involved in the 291 synthesis of amides in flowers (Grienenberger et al. 2009; Palmett et al., 2015; Li et al. 2021). 292 We identified sequences from bean, red clover, and Medicago truncatula belonging to this 293 subclade, which could have similar function. However, considering the occurrence of both 294 convergent and divergent evolution in the BAHD acyltransferases, it is difficult to predict their 295 role. The other subclade contains the red clover TpHMT and TpHDT (Sullivan 2009; Sullivan Field Code Changed 296 and Knollenberg 2021), and the bean PvHHHT. Although these three enzymes belong to the 297 same subclade, they form different products. TpHMT utilizes malic acid as the 298 hydroxycinnamoyl acceptor and it is essential for the accumulation of phaselic acid (caffeoyl-299 malate) and other hydroxycinnamoyl-malate esters in red clover (Sullivan and Zarnowski 2011). Field Code Changed 300 TpHDT utilizes L-tyrosine and L-DOPA (L-3,4-dihydroxyphenylalanine) as hydroxycinnamoyl

302	acceptors and has a role in the synthesis of clovamide and related amides (Sullivan and	 Formatted: English (US)
303	Knollenberg 2021). The role of phaselic acid and clovamide in plants is not fully understood, but	
304	they are oxidized by polyphenol oxidases (PPO), generating products that may be involved in the	
305	defense against insect herbivores and pathogens (Thipyapong, Hunt, and Steffens 2004).	Formatted: English (US)
306	PvHHHT utilizes tetrahydroxyhexanedioic acid acceptors mucic and saccharic acid, forming	
307	hydroxycinnamoyl esters with them (Sullivan 2017). The role of these compounds has not yet	Formatted: English (US)
308	been elucidated, but they also may be involved in biotic/abiotic stress responses (Elliger et al.	Formatted: English (US)
309	1981).	
1 310		
311	Comparing the amino acid sequences, PvHHHT shares 70% similarity (54% identity) with	
312	TpHMT and 71% similarity (56% identity) with TpHDT, while TpHMT and TpHDT share 83%	
1 313	similarity (72% identity) (Fig. 3). Even though the three enzymes are similar with respect to	
314	amino acid sequence, they utilize different acyl acceptor substrates and make distinct products.	
315	This functional divergence is common in the BAHD acyltransferase family (Kruse et al. 2022).	 Field Code Changed
316	On the other hand, there are also examples of BAHD enzymes with little sequence similarity that	
317	have the same substrate specificity. Two ferulate monolignol transferases, one from Angelica	
318	sinensis Oliv. and another from rice, share only 20% similarity. The enzyme from the eudicot A.	 Deleted: ,
319	sinensis Oliv. belongs to clade IIIa, whereas the one from rice belongs to clade Va (Karlen et al.	 Formatted: English (US)
320	2016). Also, the EpHMT enzyme from <i>Echinacea purpurea</i> belongs to the HCT/HQT subclade	
1 321	of clade Vb (Fu et al. 2022), sharing only 55% similarity (36% identity) with the red clover	 Field Code Changed
322	HMT.	
323		

325 Although we have measured HMT activity in leaves of bean (Sullivan 2017), an HMT gene has Field Code Changed 326 yet to be identified. The other bean proteins in the HMT/HDT/HHHT subclade are potential 327 candidates. However, considering the many cases of functional divergence and convergent 328 evolution in the BAHD family, the bean HMT enzyme could also belong to another clade of 329 BAHD acyltransferases. 330 331 Expression profiling and promoter analysis. 332 333 To investigate the expression pattern of *Pvhhht* in distinct tissues and conditions, we retrieved 334 data from the P. vulgaris Gene Expression Atlas (O'Rourke et al. 2014), which provides gene Field Code Changed 335 expression levels obtained from seven tissues at distinct developmental stages and under three 336 nitrogen treatments. The Pvhhht gene was highly expressed in leaves and flowers, a finding 337 consistent with isolation of the cDNA from young leaves (Sullivan 2017). Furthermore, the Field Code Changed 338 highest levels of expression were in leaves 21 days after inoculation with an ineffective nitrogen-339 fixing strain of rhizobia, which suggests an upregulation of Pvhhht under the condition of 340 nitrogen deficiency (Fig. 4A). We also analyzed data from another work (Ayyappan et al. 2015) Field Code Changed 341 that identified differentially expressed genes in bean leaves inoculated with the fungal rust 342 Uromyces appendiculatus. In this dataset, Pvhhht was upregulated 84 hours after inoculation 343 (Fig. 4B). Taken together with the fact that many BAHD enzymes are involved in the 344 biosynthesis of specialized metabolites, and considering the structure of PvHHHT products, 345 these results support a potential role of this enzyme in abiotic and biotic stress responses. 346

347	We also looked for stress responsive cis-elements in the promoter region of Pvhhht. Using the	 Deleted:
1 348	NewPlace database (Higo et al. 1999), we found elements related to abiotic stress, hormone, and	 Field Code Changed
349	pathogen responses (Fig. 5), Of note, there were two nodulation-related cis-elements (called	 Formatted: English (US)
350	OSE1 ROOTNODULE and OSE2 ROOTNODULE) found in the promoter, even though Pvhhht	
351	is not expressed in the nodules based on the Gene Expression Atlas data (O'Rourke et al. 2014)	 Field Code Changed
352	(Fig. 4A). A closer look at these motifs, specifically OSE2 ROOTNODULE, showed that it is	
353	oriented on the minus (-) strand approximately 133 base pairs upstream of the transcriptional	
354	start of Pvhhht. The orientation and sequence of this motif ('AAGAG') is an exact match to half	
355	of the Nitrogen Response Element (NRE), which is the binding site of NIN-Like Proteins (NLPs)	
356	(Jiang et al. 2021). Furthermore, there is a possible match to the other half of the NRE 30 bp	 Deleted: base-pairs
357	upstream of the 'AAGAG' motif, indicating that there may indeed be an NRE cis-element in the	 Formatted: English (US)
358	promoter of this gene that binds NLPs. While some NLPs have been shown to be important in	
359	the legume-rhizobium symbiosis, they are broadly responsive to the nitrogen status of the plant	
360	(Jiang et al. 2021; Konishi and Yanagisawa 2013), which may be important for <i>Pvhhht</i>	 Formatted: English (US)
361	expression since it is upregulated under nitrogen deficiency conditions.	
362	onpression since we aprogramme managem controller, continues.	
363	The role of PvHHHT products, hydroxycinnamoyl glucaric and saccharic esters, is still not clear.	
364	However, many of the characterized enzymes belonging to clade Vb are involved in the	
365	synthesis of phenolic metabolites known to be related to plant defense (Roumani et al. 2021;	
366	Qiao et al. 2024). In tomato, it has been suggested that caffeoyl glucaric acid esters have a role in	
367	pathogen response, as these inhibited the growth of tomato fruitworm (Heliothis zea) (Elliger et	 Formatted: English (US)
368	al. 1981). Another study showed that a caffeoyl glucaric acid derivative from the plant	
369	Leontopodium alpinum Cass. has pronounced antioxidative properties in vitro (Schwaiger et al,	

372	2005). Together, these data (the HHHT products, the gene expression profile, and the <i>cis</i> -	
373	elements identified,) suggest PvHHHT participates in pathogen or abiotic stress responses, and	
374	provides a foundation for further work to address its role <i>in planta</i> .	Formatted: Font: Italic
375		
376	Determination of HHHT kinetic parameters.	
377		
378	To analyze the enzymatic properties of HHHT, a histidine-tagged, codon-optimized version was	
379	expressed in E. coli and purified by immobilized metal affinity chromatography (IMAC) (Fig. 6).	
380	A large portion of the expressed protein was insoluble despite induction at 18 °C, which has been	
381	shown to enhance production of soluble protein for at least some hydroxycinnamoyl transferases	
382	(Sullivan 2009). Nonetheless, soluble protein was apparent in the induced culture lysate and	Formatted: English (US)
383	could be greatly enriched by IMAC. Migration of the induced and purified protein on SDS-	
384	PAGE was consistent with the predicted molecular mass of 52.6 kDa for the histidine-tagged	
385	HHHT. A major protein that copurified with HHHT (molecular weight of approximately 70 kDa)	
386	might be DnaK, which has been reported to copurify with histidine-tagged proteins on IMAC	
387	(Rial and Ceccarelli 2002) The resulting HHHT preparation was used in kinetic analyses using p-	Formatted: English (US)
388	coumaroyl-, caffeoyl-, and feruloyl-CoA donors and saccharic and mucic acid acceptors.	
389		
390	Initial reaction rates for HHHT were determined by measuring the release of free CoA	
391	spectrophotometrically using DTNB as previously described (Sullivan 2023). To rule out any	Formatted: English (US)
392	promiscuous reaction of DTNB with other components, we performed control reactions lacking	
393	either the donor or acceptor substrate, with the addition of enzyme and no substrate, and without	

394 added enzyme. We saw no significant net change in the absorbance at 412 nm for any of these 395 controls. 396 397 Impact of pH on reaction rate was first determined in reactions with 20 µM p-coumaroyl-CoA 398 donor and 2 mM saccharic acid as the acceptor at pH values between 6.5 and 8.0 (Table 3). 399 Higher pH values were not tested as the CoA thioester becomes unstable at higher pH. Although 400 the reaction rate was highest at pH 8.0, the rate at pH 7.5 was nearly as high (94%). 401 Consequently, reactions to determine kinetic parameters for HHHT were carried out at pH 7.5 402 since the hydroxycinnamoyl-CoA donors are both more stable under this condition and have a 403 lower extinction coefficient at 412 nm at this pH compared to pH 8.0, making rate measurements 404 using DTNB simpler. 405 406 Results of the kinetic analysis are shown in Fig. 7 and Table 4. K_M values for hydroxycinnamoyl 407 donors were in the range from 5-20 µM, a range slightly higher than that reported for red clover 408 HDT (Sullivan and Knollenberg), but lower than that reported for red clover HMT and HST 409 (hydroxycinnamoyl-CoA:shikimate hydroxycinnamoyl transferase) (Sullivan and Zarnowski 410 2011; Sullivan 2023). K_M values for p-coumaroyl- and feruloyl-CoA donors were similar for 411 either acceptor substrate, but that of caffeoyl-CoA was markedly (>three-fold) higher with mucic 412 acid as acceptor compared with saccharic acid. Values for k_{cat} were two- to four-fold higher with 413 saccharic acid as the acceptor, which also drove catalytic efficiency (as $k_{\text{cat}}/K_{\text{M}}$) to be higher for the saccharic acid acceptor compared to the mucic acid acceptor. 414 415

Formatted: English (US)

K_M values for saccharic and mucic acid acceptors were in the 2.5 to 5 mM range for both 416 417 acceptors and varied depending on which donor was being used. Values for k_{cat} when acceptors 418 were the variable substrate were nearly the same for each donor-acceptor combination as when 419 donors were the variable substrate for each donor-acceptor combination. This is expected since 420 this value represents turnover when substrates are at saturating levels. Because $K_{\rm M}$ values for the 421 acceptors are high relative to those of the donors, catalytic efficiencies (as $k_{cat}/K_{\rm M}$) for these 422 measurements are several hundred-fold lower than when donors were used as the variable 423 substrate. Similar to measurements made with donors as the variable substrate, kcat/K_M were two-424 to four-fold lower for mucic acid than for saccharic acid. Although the higher catalytic efficiency 425 observed for saccharic acid as an acceptor is consistent with the observation that 426 hydroxycinnamoyl-saccharic acid esters predominate over mucic acid esters in bean leaves 427 (Sullivan, 2017), acceptor concentration in vivo, currently unknown, would almost certainly also 428 play a role in the relative accumulation of products in vivo, especially given the modest 429 difference in magnitude of catalytic efficiencies. 430 431 Also, since the Km values for the acyl acceptors were relatively larger and considering that 432 divalent metals commonly chelate carboxylates in active sites (Larsen et al. 1996), we tried 433 adding Mg⁺² to the reaction, but this had no impact on the reaction rates. 434

Formatted: English (US)

Protein structure model and molecular docking.

435

436

To investigate the interactions between HHHT and the acyl group acceptor ligands (mucic and saccharic acid) in the active site, and gain insights about the higher catalytic efficiency of

439 saccharic acid in comparison to mucic acid, we downloaded a predicted protein structure model 440 of HHHT from AlphaFold and performed molecular docking of the ligands into the enzyme. The 441 model had a high to very high confidence score for most of the residues. Molprobity results 442 validated the structure. The predicted HHHT structure has two chloramphenicol 443 acetyltransferase-like domains (residues 1 to 207 and residues 214 to 448) and consists of 14 444 beta-sheets and 19 alpha-helices (Fig. 8). The two-domain 3-D structure is similar to that of other 445 BAHD acyltransferases elucidated using X-ray crystallography (Lallemand et al. 2012; Ma et al. 446 2005; Walker et al. 2013). The active site motif HXXXD is in a region predicted with a very 447 high-confidence score by AlphaFold. Nevertheless, some regions close to the active site, 448 predicted with a high confidence score, carry some amino acids that could participate in 449 conformational changes or interactions with other components, which cannot be predicted by 450 AlphaFold. For example, the region from amino acids 345-351 contain a solvent exposed 451 arginine that could form salt bridges. The region from residues 351-375 line the active site and 452 carry a solvent exposed cysteine (Cys-359), which could be involved in the formation of 453 different conformations or stabilizing quaternary structure via disulfide bridges. There are also 454 other residues such as Glu-354, Asp-358, Arg-361, Arg-362, that could form salt bridges, and 455 Met-365 that could form disulfide bonds. Therefore, this region is likely flexible. 456 457 After performing the molecular docking of the mucic acid and saccharic acid structures into the 458 protein model, nine conformations were obtained for each ligand (Table 5). The lowest binding 459 energies obtained for saccharic and mucic acid conformations were very similar, which suggests 460 there is not a markedly higher affinity for one substrate over the other. This is also consistent 461 with the measured $K_{\rm M}$ values for the acceptors, which were very similar for saccharic and mucic

Field Code Changed

462 acid. The lowest energy conformations (number 1 in the table) were visualized to analyze the 463 HHHT active site (Fig. 9). The protein residues His 150 and Gly 155, which are part of the 464 HXXXD motif, form interactions with both mucic and saccharic acid. It has been shown for 465 many BAHD acyltransferases that the histidine in this motif is essential for activity. In multiple 466 mutagenesis experiments, replacement of this histidine with alanine abolishes enzyme activity 467 (Lallemand et al. 2012; Walker et al. 2016; Bayer, Ma, and Stöckigt 2004). It has been proposed Formatted: English (US) 468 that this catalytic histidine serves as a general base, abstracting a proton from the acyl acceptor 469 substrate (Levsh et al. 2016; Ma et al. 2005). For sorghum HCT (Walker et al. 2016), it was Formatted: English (US) Formatted: English (US) 470 proposed that the imidazole atom from His 152 is properly oriented with the aid of Thr 36 to 471 abstract a proton from shikimic acid. This enables a nucleophilic attack of the shikimate 472 hydroxyl on the thioester carbonyl of hydroxycinnamoyl-CoA. Here, with the docking results, 473 we also found Thr 35 in the active site, next to His 150 that could be aiding the proton 474 abstraction from a hydroxyl group of mucic or saccharic acid. It was also found for SbHCT that a 475 Trp in position 384 and an Arg in position 371 are important for catalytic activity and are likely 476 involved in the binding of the shikimate molecule. We also found Trp in position 386 and Arg in 477 position 414 of HHHT interacting with the substrates in our docking analysis. Another amino 478 acid we found interacting with mucic and saccharic acid was Tyr 408. 479 480 We also investigated potential binding sites for the hydroxycinnamoyl ligands. Since these 481 Formatted: English (US) molecules are large, which represents a challenge for accurate computational docking (Devaurs 482 et al. 2019), we did not obtain satisfactory results using the whole ligand. Therefore, we used the 483 N-acetyl-S-hydroxycinnamoyl-cysteamine portion for the analysis. We obtained nine 484 conformations for each acyl donor ligand (Table 6). The lowest binding energies for p-

485 coumaroyl, caffeoyl and feruloyl ligands were all similar, which is consistent with the similar 486 donor substrate K_M values. In these conformations, they were all placed in the same region as mucic and saccharic acid (Figure 10), which supports the identified binding site. The acyl-donors 487 488 formed interactions with Thr 37, Gly 155 and Arg 414. 489 All the putative residues identified through docking as interacting with ligands are conserved in 490 491 red clover HMT and HDT as well, with exception of Thr 35 which is replaced by a valine in 492 HDT (Figure 3), suggesting they are important for transferase activity. 493 494 In our analysis, we were not able to determine to which hydroxyl group of mucic or saccharic 495 acid the hydroxycinnamate is transferred. Nonetheless, for the imidazole nitrogen of His150 to 496 abstract a proton from the hydroxyl group, the distance between the atoms has to be less than 4 Å 497 (Harris and Mildvan 1999). From the docking (Figure 9), for mucic acid, hydroxyl groups in C4 Formatted: English (US) 498 and C5 are positioned 3.0 and 3.3 Å, respectively, from the imidazole nitrogen, which would 499 allow a proton transfer. For saccharic acid, hydroxyl groups in C2, C3, and C4 are 3.0, 3.0. and 500 3.3Å, respectively, from the imidazole nitrogen, and could be involved in the proton transfer 501 Formatted: Font: Italic reaction. In previous work (Sullivan, 2017), we analyzed PvHHHT *in vitro* reaction products 502 using LC-MS and observed multiple peaks. We detected the formation of three to four different 503 products for the *in vitro* reaction of pCA, CA, or FA-coA with saccharic acid. On the other hand, Formatted: Font: Italic 504 we detected only one product for the reaction of pCA or CA with mucic acid, and two products 505 for FA with mucic acid. We considered this to be likely the result of non-enzymatic 506 intramolecular transesterification reactions between the hydroxycinnamoyl-ester and the other 507 hydroxyl groups of the molecule. However, the larger diversity of products identified for the

reactions with saccharic acid <u>ys.</u> mucic acid, together with the docking results showing proximity	Deleted: versus
of multiple hydroxyl groups to the imidazole N of His-150, suggest that besides	
transesterification reactions it may be that HHHT can acylate different sites of the	
tetrahydroxyhexanedioic acids molecules. BAHD transferases catalyzing multisite acylation	
reactions have been previously reported. Arabidopsis thaliana AtSHT and AtSDT, also	
belonging to clade Vb (Figure 2), substitute multiple N positions of spermidine (Wang et al.	Deleted:
2021). Other spermidine hydroxycinnamoyl transferases involved in the synthesis of tri-	
substituted spermidine or tetra-substituted spermine were identified in Malus domestica	
(MdSHT) and Cichorium intybus (CiSHT) (Elejalde-Palmett et al. 2015; Delporte et al. 2018).	Formatted: English (US)
Also, a saponine acetyltransferase from Astragalus membranaceus, AmAT7-3, acetylates C3'-O	
and C4'-O of xylose of the compound astragaloside IV (Wang et al. 2023). Therefore, PvHHHT	Formatted: English (US)
could also be a multi-site transferase.	
Site-directed mutagenesis and enzymatic analysis	
To test whether the interacting residues identified through the structure and docking analysis are	
important for substrate binding or catalysis, we used site-directed mutagenesis to replace each of	
the residues Thr 35, His 150, Trp 386, and Arg 414 with alanine, and evaluated transferase	Deleted: ,
activity for the reaction with 100 μ M saccharic acid and 20 mM p -coumaric acid. All mutants	
had very little activity, ranging from 2 to 8 % of that of the native wild type protein (Figure 11).	Deleted:
These results support the docking analysis and show that these residues are important for	
catalysis.	
	of multiple hydroxyl groups to the imidazole N of His-150, suggest that besides transesterification reactions it may be that HHHT can acylate different sites of the tetrahydroxyhexanedioic acids molecules. BAHD transferases catalyzing multisite acylation reactions have been previously reported. <i>Arabidopsis thaliana</i> AtSHT and AtSDT, also belonging to clade Vb (Figure 2), substitute multiple N positions of spermidine (Wang et al. 2021). Other spermidine hydroxycinnamoyl transferases involved in the synthesis of trisubstituted spermidine or tetra-substituted spermine were identified in Malus domestica (MdSHT) and Cichorium intybus (CiSHT) (Elejalde-Palmett et al. 2015; Delporte et al. 2018). Also, a saponine acetyltransferase from <i>Astragalus membranaceus</i> , AmAT7-3, acetylates C3'-O and C4'-O of xylose of the compound astragaloside IV (Wang et al. 2023). Therefore, PvHHHT could also be a multi-site transferase. Site-directed mutagenesis and enzymatic analysis To test whether the interacting residues identified through the structure and docking analysis are important for substrate binding or catalysis, we used site-directed mutagenesis to replace each of the residues Thr 35, His 150, Trp 386, and Arg 414 with alanine, and evaluated transferase activity for the reaction with 100 μM saccharic acid and 20 mM <i>p</i> -coumaric acid. All mutants had very little activity, ranging from 2 to 8 % of that of the native wild, type protein (Figure 11). These results support the docking analysis and show that these residues are important for

The impact of the H150A mutation supports the important catalytic role of this residue, which is part of the HXXXD active site motif. In their work with SbHCT, Walker et al. 2016 also found very little activity for a T36A and a R371A mutant. Also, R386 in the active site of *Arabidopsis*

thaliana HCT was shown to be important for substrate specificity (Levsh et al., 2016).

Formatted: Font: Italic

Conclusions

535

536

537

538

539

540

541

542

543

544

545

546

547

548

549

550

551

552

553

554

555

556

557

Like other clade Vb BAHD transferases, expression pattern and promoter analysis suggest a role of HHHT in defensive responses. The highest level of expression appears to be in leaves of plants inoculated with an ineffective strain of nitrogen-fixing rhizobia (Fig. 4A). HHHT was also upregulated in response to inoculation with a fungal pathogen (Fig. 4B). Further, numerous potential stress-responsive promoter elements are present in the upstream region of the gene (Fig. 5). Kinetic parameters for both donor CoA substrates (μ M $K_{\rm M}$) and acceptor substrates (μ M $K_{\rm M}$) are in the range of those reported for other hydroxycinnamoyl transferases that have been biochemically characterized (Table 4). The enzyme appears to be more efficient in using saccharic acid compared to mucic acid, even though they had similar binding poses when docked into the active site and their $K_{\rm M}$ did not vary substantially. This suggests that factors other than acceptor substrate affinity contribute to the difference in efficiency between the two substrates. For example, mucic acid may be less favorably oriented in the active site for ester formation relative to saccharic acid. Furthermore, proximity of multiple hydroxyl groups of saccharic acid to the imidazole N of the active site His may explain the formation of multiple products previously attributed to intramolecular transesterifications. The structure and active site data here, along with kinetic parameters of the enzyme, should contribute to the growing body of such 558 data that might ultimately provide a better understanding of the relationship of the 3-D structure 559 of BAHD transferases to their substrate specificity, which should allow better prediction of 560 enzyme function from primary amino acid sequence. These data could further provide the basis 561 for rational design of BAHD enzymes to produce desired and novel products. 562 563 Acknowledgments 564 565 We wish to thank Joe Jez for useful discussions on structure modeling and active site docking. We also thank Laurie Reinhardt for helpful comments on the manuscript. All opinions expressed 566 in this paper are the author's and do not necessarily reflect the policies and views of USDA, 567 DOE, or ORAU/ORISE. Mention of trade names or commercial products in this article is solely 568 569 for the purpose of providing specific information and does not imply recommendation or 570 endorsement by the U.S. Department of Agriculture. 571 Formatted: English (US) References 572 573 574 Ayyappan, Vasudevan, Venu Kalavacharla, Jyothi Thimmapuram, Ketaki P Bhide, 575 Venkateswara R Sripathi, Tomasz G Smolinski, Muthusamy Manoharan, Yaqoob 576 Thurston, Antonette Todd, and Bruce Kingham. 2015. "Genome-Wide Profiling of Histone Modifications (H3K9 Me2 and H4K12 Ac) and Gene Expression in Rust 577 578 (Uromyces appendiculatus) Inoculated Common Bean (Phaseolus vulgaris L.)." Plos One 10 (7). https://doi.org/10.1371/journal.pone.0132176. 579 Field Code Changed 580 Bartley, Laura E., Matthew L. Peck, Sung-Ryul S.-R. Kim, Berit Ebert, Chithra Manisseri, Dawn M. Chiniquy, Robert Sykes, Lingfang Gao, Carsten Rautengarten, Miguel E. Vega-581 582 Sánchez, Peter I. Benke, Patrick E. Canlas, Peijian Cao, Susan Brewer, Fan Lin, Whitney 583 L. Smith, Xiaohan Zhang, Jay D. Keasling, Rolf E. Jentoff, Steven B. Foster, Jizhong 584 Zhou, Angela Ziebell, Gynheung An, Henrik V. Scheller, and Pamela C. Ronald. 2013. 585 "Overexpression of a BAHD Acyltransferase, OsAt10, Alters Rice Cell Wall 586 Hydroxycinnamic Acid Content and Saccharification." Plant Physiology, 161 (4): 1615-Field Code Changed 33. https://doi.org/10.1104/pp.112.208694. 587 Field Code Changed 588 Bayer, Anja, Xueyan Ma, and Joachim Stöckigt. 2004. "Acetyltransfer in Natural Product Formatted: English (US) 589 Biosynthesis—Functional Cloning and Molecular Analysis of Vinorine Synthase."

590	Bioorganic & Medicinal Chemistry 12 (10): 2787–95.	
591	https://doi.org/10.1016/j.bmc.2004.02.029.	
592	Bontpart, Thibaut, Véronique Cheynier, Agnès Ageorges, and Nancy Terrier. 2015. "BAHD or	Field Code Changed
593	SCPL Acyltransferase? What a Dilemma for Acylation in the World of Plant Phenolic	
594	Compounds." New Phytologist 208 (3): 695–707. https://doi.org/10.1111/nph.13498.	Field Code Changed
595	Constabel, C. Peter, and Raymond Barbehenn. 2008. "Defensive Roles of Polyphenol Oxidase in	Field Code Changed
596	Plants." In <i>Induced Plant Resistance to Herbivory</i> , edited by Andreas Schaller, 253–70.	Field Code Changed
597	Dordrecht: Springer Netherlands. https://doi.org/10.1007/978-1-4020-8182-8_12.	Field Code Changed
598 500	Delporte, Marianne, Guillaume Bernard, Guillaume Legrand, Björn Hielscher, Arnaud Lanoue,	Field Code Changed
599	Roland Molinié, Caroline Rambaud, David Mathiron, Sébastien Besseau, Nicole Linka,	Formatted: English (US)
600	Jean-Louis Hilbert, and David Gagneul. 2018. "A BAHD Neofunctionalization Promotes	
601	Tetrahydroxycinnamoyl Spermine Accumulation in the Pollen Coat of the Asteraceae	
602	Family." Journal of Experimental Botany 69 (22): 5355–71.	
603	https://doi.org/10.1093/jxb/ery320.	
604	Devaurs, Didier, Dinler A. Antunes, Sarah Hall-Swan, Nicole Mitchell, Mark Moll, Gregory	
605	Lizée, and Lydia E. Kavraki. 2019. "Using Parallelized Incremental Meta-Docking Can	
606	Solve the Conformational Sampling Issue When Docking Large Ligands to Proteins."	
607	BMC Molecular and Cell Biology 20 (1): 42. https://doi.org/10.1186/s12860-019-0218-z.	
608	Eberhardt, Jerome, Diogo Santos-Martins, Andreas F. Tillack, and Stefano Forli. 2021.	Field Code Changed
609 610	"AutoDock Vina 1.2.0: New Docking Methods, Expanded Force Field, and Python	Field Code Changed
611	Bindings." Journal of Chemical Information and Modeling, 61 (8): 3891–98. https://doi.org/10.1021/acs.jcim.1c00203.	Field Code Changed
612	Elejalde-Palmett, Carolina, Thomas Dugé De Bernonville, Gaëlle Glevarec, Olivier Pichon,	Formatted: English (US)
613	Nicolas Papon, Vincent Courdavault, Benoit St-Pierre, Nathalie Giglioli-Guivarc'h,	Formatted: English (US)
614	Arnaud Lanoue, and Sébastien Besseau. 2015. "Characterization of a Spermidine	
615	Hydroxycinnamoyltransferase in <i>Malus domestica</i> Highlights the Evolutionary	
616	Conservation of Trihydroxycinnamoyl Spermidines in Pollen Coat of Core	
617	Eudicotyledons." <i>Journal of Experimental Botany</i> 66 (22): 7271–85.	
618	https://doi.org/10.1093/jxb/erv423.	
619	Elliger, C. A., Y. Wong, B. G. Chan, and A. C. Waiss. 1981. "Growth Inhibitors in Tomato	
620	(Lycopersicon) to Tomato Fruitworm (Heliothis zea)." Journal of Chemical Ecology 7	
621	(4): 753–58. https://doi.org/10.1007/BF00990307.	
622	Fanelli, Amanda, and Michael Sullivan. 2022. "Tools for Protein Structure Prediction and for	Field Code Changed
623	Molecular Docking Applied to Enzyme Active Site Analysis: A Case Study Using a	
624	BAHD Hydroxycinnamoyltransferase." <i>Methods in Enzymology</i> , 683: 41-79.	Field Code Changed
625	https://doi.org/10.1016/BS.MIE.2022.10.004.	
626	Fu, Rao, Pingyu Zhang, Ge Jin, Shuo Wei, Jiang Chen, Jin Pei, and Yang Zhang. 2022.	Field Code Changed
627	"Substrate Promiscuity of Acyltransferases Contributes to the Diversity of	
628 629	Hydroxycinnamic Acid Derivatives in Purple Coneflower." <i>Plant Journal</i> 110 (3): 802–	Field Code Changed
630	13. https://doi.org/10.1111/tpj.15704. Gouy, Manolo, Eric Tannier, Nicolas Comte, and David P. Parsons. 2021. "Seaview Version 5:	Field Code Changed
631	A Multiplatform Software for Multiple Sequence Alignment, Molecular Phylogenetic	Field Code Changed
632	Analyses, and Tree Reconciliation." <i>Methods in Molecular Biology</i> 2231:241–60.	Field Code Changed
		Field Code Changed

633	https://doi.org/10.1007/978-1-0716-1036-7 15.		
634	Grienenberger, Etienne, Sébastien Besseau, Pierrette Geoffroy, Delphine Debayle, Dimitri		Field Code Changed
635	Heintz, Catherine Lapierre, Brigitte Pollet, Thierry Heitz, and Michel Legrand. 2009. "A		
636	BAHD Acyltransferase Is Expressed in the Tapetum of Arabidopsis Anthers and Is		
637	Involved in the Synthesis of Hydroxycinnamoyl Spermidines." The Plant Journal 58 (2):		Field Code Changed
638	246–59. https://doi.org/10.1111/j.1365-313X.2008.03773.x.	***************************************	Field Code Changed
639	Harris, Thomas K., and Albert S. Mildvan. 1999. "High-Precision Measurement of Hydrogen		Formatted: English (US)
640	Bond Lengths in Proteins by Nuclear Magnetic Resonance Methods." Proteins:		
641	Structure, Function, and Bioinformatics 35 (3): 275–82.		
642	https://doi.org/10.1002/(sici)1097-0134(19990515)35:3<275::aid-prot1>3.0.co;2-v.		
643	Higo, Kenichi, Yoshihiro Ugawa, Masao Iwamoto, and Tomoko Korenaga. 1999. "Plant Cis-		Field Code Changed
644	Acting Regulatory DNA Elements (PLACE) Database: 1999." Nucleic Acids Research		Field Code Changed
645	27 (1): 297–300. https://doi.org/10.1093/nar/27.1.297.	***************************************	Field Code Changed
646	Hoffmann, L, S Besseau, P Geoffroy, C Ritzenthaler, D Meyer, C Lapierre, B Pollet, and M		Field Code Changed
647	Legrand. 2005. "Acyltransferase-Catalysed <i>p</i> -Coumarate Ester Formation Is a Committed		
648	Step of Lignin Biosynthesis." Plant Biosystems - An International Journal Dealing with		Field Code Changed
649	All Aspects of Plant Biology 139 (1): 50–53.		Field Code Changed
650	https://doi.org/10.1080/11263500500054992.		
651	Jiang, Suyu, Marie-Françoise Jardinaud, Jinpeng Gao, Yann Pecrix, Jiangqi Wen, Kirankumar		Formatted: English (US)
652	Mysore, Ping Xu, Carmen Sanchez-Canizares, Yiting Ruan, Qiujiu Li, Meijun Zhu, Fuyu		
653	Li, Ertao Wang, Phillip S. Poole, Pascal Gamas, and Jeremy D. Murray. 2021. "NIN-like		
654	Protein Transcription Factors Regulate Leghemoglobin Genes in Legume Nodules."		
655	Science 374 (6567): 625–28. https://doi.org/10.1126/science.abg5945.		
656	Jisna, V. A., and P. B. Jayaraj. 2021. "Protein Structure Prediction: Conventional and Deep		Field Code Changed
657	Learning Perspectives." <i>Protein Journal</i> 40 (4): 522–44. https://doi.org/10.1007/s10930-	Santa Caraca	Field Code Changed
658	021-10003-y.	*******	Field Code Changed
659 660	Kalyaanamoorthy, Subha, Bui Quang Minh, Thomas K. F. Wong, Arndt von Haeseler, and Lars S. Jermiin. 2017. "ModelFinder: Fast Model Selection for Accurate Phylogenetic		Field Code Changed
661	Estimates." <i>Nature Methods</i> , 14 (6): 587–89. https://doi.org/10.1038/nmeth.4285.		Field Code Changed
662	Karlen, Steven D, Chengcheng Zhang, Matthew L. Peck, Rebecca A Smith, Dharshana		Field Code Changed
663	Padmakshan, Kate E Helmich, Heather C A Free, Seonghee Lee, Bronwen G. Smith,	***************************************	Formatted: English (US)
664	Fachuang Lu, John C. Sedbrook, Richard Sibout, John H. Grabber, Troy M. Runge,		Formatted. Eligibil (US)
665	Kirankumar S. Mysore, Philip J. Harris, Laura E. Bartley, and John Ralph. 2016.		
666	"Monolignol Ferulate Conjugates Are Naturally Incorporated into Plant Lignins." <i>Science</i>		
667	Advances 2:1–9. https://doi.org/10.1126/sciadv.1600393.		
668	Konishi, Mineko, and Shuichi Yanagisawa. 2013. "Arabidopsis NIN-like Transcription Factors		
669	Have a Central Role in Nitrate Signalling." <i>Nature Communications</i> 4 (1): 1617.		
670	https://doi.org/10.1038/ncomms2621.		
671	Kruse, Lars H., Austin T. Weigle, Mohammad Irfan, Jesús Martínez-Gómez, Jason D. Chobirko,		Field Code Changed
672 673	Jason E. Schaffer, Alexandra A. Bennett, Chelsea D. Specht, Joseph M. Jez, Diwakar		
674	Shukla, and Gaurav D. Moghe. 2022. "Orthology-Based Analysis Helps Map Evolutionary Diversification and Predict Substrate Class Use of BAHD		
675	Acyltransferases." <i>The Plant Journal</i> , 111 (5): 1453–68.		Field Code Changed
676	https://doi.org/10.1111/tpj.15902.	C. C.	Field Code Changed
0.0	mapon density to it it is placed.		Fich Cour Changen

677	Lallemand, L. A., C. Zubieta, S. G. Lee, Y. Wang, S. Acajjaoui, J. Timmins, S. McSweeney, J.	Field Code Changed
678	M. Jez, J. G. McCarthy, and A. A. McCarthy. 2012. "A Structural Basis for the	
679	Biosynthesis of the Major Chlorogenic Acids Found in Coffee." <i>Plant Physiology</i> , 160	Field Code Changed
680	(1): 249–60. https://doi.org/10.1104/pp.112.202051.	Field Code Changed
681	Larsen, Todd M., Joseph E. Wedekind, Ivan Rayment, and George H. Reed. 1996. "A	
682	Carboxylate Oxygen of the Substrate Bridges the Magnesium Ions at the Active Site of	
683	Enolase: Structure of the Yeast Enzyme Complexed with the Equilibrium Mixture of 2-	
684	Phosphoglycerate and Phosphoenolpyruvate at 1.8 Å Resolution." Biochemistry 35 (14):	
685	4349–58. https://doi.org/10.1021/bi952859c.	
686	Letunic, Ivica, and Peer Bork. 2021. "Interactive Tree Of Life (iTOL) v5: An Online Tool for	Field Code Changed
687	Phylogenetic Tree Display and Annotation." Nucleic Acids Research 49 (W1): W293-96.	Field Code Changed
688	https://doi.org/10.1093/nar/gkab301.	Field Code Changed
689	Levsh, Olesya, Ying Chih Chiang, Chun Fai Tung, Joseph P. Noel, Yi Wang, and Jing Ke Weng.	Formatted: English (US)
690	2016. "Dynamic Conformational States Dictate Selectivity toward the Native Substrate in)
691	a Substrate-Permissive Acyltransferase." Biochemistry 55 (45): 6314-26.	
692	https://doi.org/10.1021/acs.biochem.6b00887.	
693	Luo, Jie, Yasutaka Nishiyama, Christine Fuell, Goro Taguchi, Katherine Elliott, Lionel Hill,	Field Code Changed
694	Yoshikazu Tanaka, Masahiko Kitayama, Mami Yamazaki, Paul Bailey, Adrian Parr,	
695	Anthony J. Michael, Kazuki Saito, and Cathie Martin. 2007. "Convergent Evolution in	
696	the BAHD Family of Acyl Transferases: Identification and Characterization of	
697	Anthocyanin Acyl Transferases from Arabidopsis Thaliana." Plant Journal, 50 (4): 678-	Field Code Changed
698	95. https://doi.org/10.1111/j.1365-313X.2007.03079.x.	Field Code Changed
699	Ma, Xueyan, Juergen Koepke, Santosh Panjikar, Günter Fritzsch, and Joachim Stöckigt. 2005.	Field Code Changed
700	"Crystal Structure of Vinorine Synthase, the First Representative of the BAHD	(the constant
701	Superfamily." The Journal of Biological Chemistry 280 (14): 13576–83.	Field Code Changed
702	https://doi.org/10.1074/jbc.M414508200.	Field Code Changed
703	Moghe, Gaurav, Lars H. Kruse, Maike Petersen, Federico Scossa, Alisdair R. Fernie, Emmanuel	Field Code Changed
704	Gaquerel, and John C. D'Auria. 2023. "BAHD Company: The Ever-Expanding Roles of	
705	the BAHD Acyltransferase Gene Family in Plants." Annual Review of Plant Biology 74	Field Code Changed
706	(Volume 74, 2023): 165–94. https://doi.org/10.1146/annurev-arplant-062922-050122.	Field Code Changed
707	O'Rourke, Jamie A., Luis P. Iniguez, Fengli Fu, Bruna Bucciarelli, Susan S. Miller, Scott A.	Formatted: English (US)
708	Jackson, Philip E. McClean, Jun Li, Xinbin Dai, Patrick X Zhao, Georgina Hernandez,	
709	and Carroll P Vance. 2014. "An RNA-Seq Based Gene Expression Atlas of the Common	
710	Bean." BMC Genomics 15 (1): 866. https://doi.org/10.1186/1471-2164-15-866	
711	Potter, Simon C, Aurélien Luciani, Sean R Eddy, Youngmi Park, Rodrigo Lopez, and Robert D	Field Code Changed
712	Finn. 2018. "HMMER Web Server: 2018 Update." Nucleic Acids Research 46 (W1):	Field Code Changed
713	W200–204. https://doi.org/10.1093/nar/gky448.	Field Code Changed
714	Qiao, Dahe, Chun Yang, Xiaozeng Mi, Mengsha Tang, Sihui Liang, and Zhengwu Chen. 2024.	Formatted: English (US)
715	"Genome-Wide Identification of Tea Plant (Camellia sinensis) BAHD Acyltransferases	Formattet. English (CS)
716	Reveals Their Role in Response to Herbivorous Pests." BMC Plant Biology 24 (1): 229.	
717	https://doi.org/10.1186/s12870-024-04867-2.	
718	Ravindranath, Pradeep Anand, Stefano Forli, David S. Goodsell, Arthur J. Olson, and Michel F.	Field Code Changed
719	Sanner. 2015. "AutoDockFR: Advances in Protein-Ligand Docking with Explicitly	
720	Specified Binding Site Flexibility." <i>PLoS Computational Biology</i> 11 (12): 1–28.	Field Code Changed
721	https://doi.org/10.1371/journal.pcbi.1004586.	Field Code Changed
		<u> </u>

.. ...

722	Rial, Daniela V, and Eduardo A Ceccarelli. 2002. "Removal of DnaK Contamination during	Formatted: English (US)
723	Fusion Protein Purifications." <i>Protein Expression and Purification</i> 25 (3): 503–7.	(
	* * * * * * * * * * * * * * * * * * * *	
724	https://doi.org/10.1016/S1046-5928(02)00024-4.	
725	Roumani, Marwa, Sébastien Besseau, David Gagneul, Christophe Robin, and Romain Larbat.	
726	2021. "Phenolamides in Plants: An Update on Their Function, Regulation, and Origin of	
727	Their Biosynthetic Enzymes." Journal of Experimental Botany 72 (7): 2334-55.	
728	https://doi.org/10.1093/jxb/eraa582.	
729	Sullivan, Michael L. 2009. "A Novel Red Clover Hydroxycinnamoyl Transferase Has Enzymatic	Field Code Changed
730	Activities Consistent with a Role in Phaselic Acid Biosynthesis." <i>Plant Physiology</i> , 150	Field Code Changed
731	(4): 1866–79. https://doi.org/10.1104/pp.109.136689.	Field Code Changed
732	Sullivan, Michael L. 2017. "Identification of Bean Hydroxycinnamoyl-	Field Code Changed
733	CoA:Tetrahydroxyhexanedioate Hydroxycinnamoyl Transferase (HHHT): Use of	Field Code Changed
734	Transgenic Alfalfa to Determine Acceptor Substrate Specificity." Planta 245 (2): 397-	Field Code Changed
735	408. https://doi.org/10.1007/s00425-016-2613-4.	Field Code Changed
736	Sullivan, Michael L. 2023. "Near-Real Time Determination of BAHD Acyl-Coenzyme A	Formatted: English (US)
737	Transferase Reaction Rates and Kinetic Parameters Using Ellman's Reagent." Methods in	
738	Enzymology 683:19–39. https://doi.org/10.1016/bs.mie.2022.10.002.	
739	Sullivan, Michael L., Heather A. Green, and Julian C. Verdonk. 2021. "Engineering Alfalfa to	Field Code Changed
740	Produce 2-O-Caffeoyl-L-Malate (Phaselic Acid) for Preventing Post-Harvest Protein	(Total code changed
741	Loss via Oxidation by Polyphenol Oxidase." Frontiers in Plant Science, 11 (610399): 1–	Field Code Changed
742	16. https://doi.org/10.3389/fpls.2020.610399.	Field Code Changed
743	Sullivan, Michael L., and Ronald D. Hatfield. 2006. "Polyphenol Oxidase and O-Diphenols	
744	Inhibit Postharvest Proteolysis in Red Clover and Alfalfa." <i>Crop Science</i> , 46 (2): 662–70.	Field Code Changed
745	https://doi.org/10.2135/cropsci2005.06-0132.	Field Code Changed
746	Sullivan, Michael L., and Benjamin J. Knollenberg. 2021. "Red Clover HDT, a BAHD	Field Code Changed
747	Hydroxycinnamoyl-Coenzyme A:L-3,4-Dihydroxyphenylalanine (L-DOPA)	Field Code Changed
748	Hydroxycinnamoyl Transferase That Synthesizes Clovamide and Other N-	
749	Hydroxycinnamoyl-Aromatic Amino Acid Amides." Frontiers in Plant Science, 12	Field Code Changed
750	(November). https://doi.org/10.3389/fpls.2021.727461.	Field Code Changed
751	Sullivan, Michael L., and Robert Zarnowski. 2011. "Red Clover HCT2, a Hydroxycinnamoyl-	Field Code Changed
752	Coenzyme A: Malate Hydroxycinnamoyl Transferase, Plays a Crucial Role in	Ticiu couc changeu
753	Biosynthesis of Phaselic Acid and Other Hydroxycinnamoyl-Malate Esters in Vivo."	
754	Plant Physiology, 155 (3): 1060–67. https://doi.org/10.1104/pp.110.166793.	Field Code Changed
755	Sullivan, Michael L., and Wayne E. Zeller. 2013. "Efficacy of Various Naturally Occurring	Field Code Changed
756	Caffeic Acid Derivatives in Preventing Post-Harvest Protein Losses in Forages." <i>Journal</i>	Field Code Changed
757	of the Science of Food and Agriculture 93 (2): 219–26. https://doi.org/10.1002/jsfa.5781.	Field Code Changed
758	Thipyapong, Piyada, Michelle D. Hunt, and John C. Steffens. 2004. "Antisense Downregulation	Field Code Changed
759	of Polyphenol Oxidase Results in Enhanced Disease Susceptibility." Planta 220 (1): 105-	
760	17. https://doi.org/10.1007/s00425-004-1330-6.	Formatted: English (US)
761	Trifinopoulos, Jana, Lam Tung Nguyen, Arndt von Haeseler, and Bui Quang Minh. 2016. "W-	Field Code Changed
762	IQ-TREE: A Fast Online Phylogenetic Tool for Maximum Likelihood Analysis." <i>Nucleic</i>	Field Code Changed
763	Acids Research, 44 (W1): W232–35. https://doi.org/10.1093/nar/gkw256.	Field Code Changed
764	Tuominen, Lindsey K., Virgil E. Johnson, and Chung-Jui Jui Tsai. 2011. "Differential	Field Code Changed
765	Phylogenetic Expansions in BAHD Acyltransferases across Five Angiosperm Taxa and	Field Code Changed
766	Evidence of Divergent Expression among Populus Paralogues." <i>BMC Genomics</i> , 12 (1):	Field Code Changed
		- Note Court Changes

767 236. https://doi.org/10.1186/1471-2164-12-236. 768 Walker, Alexander M., Robert P. Hayes, Buhyun Youn, Wilfred Vermerris, Scott E. Sattler, and Field Code Changed 769 ChulHee Kang. 2013. "Elucidation of the Structure and Reaction Mechanism of Sorghum 770 Hydroxycinnamoyltransferase and Its Structural Relationship to Other Coenzyme A-771 Dependent Transferases and Synthases." Plant Physiology, 162 (2): 640-51. Field Code Changed 772 https://doi.org/10.1104/pp.113.217836. Field Code Changed 773 Walker, Kevin, Robert Long, and Rodney Croteau. 2002. "The Final Acylation Step in Taxol Formatted: English (US) 774 Biosynthesis: Cloning of the Taxoid C13-Side-Chain N-Benzoyltransferase from Taxus." 775 Proceedings of the National Academy of Sciences 99 (14): 9166–71. 776 https://doi.org/10.1073/pnas.082115799. Formatted: English (US) 777 Wang, Chengyuan, Jianxu Li, Miaolian Ma, Zhaozhu Lin, Wenli Hu, Wei Lin, and Peng Zhang. 778 2021. "Structural and Biochemical Insights Into Two BAHD Acyltransferases (AtSHT 779 and AtSDT) Involved in Phenolamide Biosynthesis." Frontiers in Plant Science 11 780 (January). https://doi.org/10.3389/fpls.2020.610118. 781 Wang, Linlin, Zhihui Jiang, Jiahe Zhang, Kuan Chen, Meng Zhang, Zilong Wang, Binju Wang, 782 Min Ye, and Xue Qiao. 2023. "Characterization and Structure-Based Protein Engineering 783 of a Regiospecific Saponin Acetyltransferase from Astragalus membranaceus." Nature 784 Communications 14 (1): 5969. https://doi.org/10.1038/s41467-023-41599-7. Formatted: English (US) Williams, Christopher J., Jeffrey J. Headd, Nigel W. Moriarty, Michael G. Prisant, Lizbeth L. 785 Videau, Lindsay N. Deis, Vishal Verma, Daniel A. Keedy, Bradley J. Hintze, Vincent B. 786 787 Chen, Swati Jain, Steven M. Lewis, W. Bryan Arendall III, Jack Snoeyink, Paul D. 788 Adams, Simon C. Lovell, Jane S. Richardson, and David C. Richardson. 2018. 789 "MolProbity: More and Better Reference Data for Improved All-Atom Structure 790 Validation." Protein Science 27 (1): 293–315. https://doi.org/10.1002/pro.3330. Field Code Changed 791 Yang, Qian, Klaus Reinhard, Emile Schiltz, and Ulrich Matern. 1997. "Characterization and Field Code Changed 792 Heterologous Expression of Hydroxycinnamoyl/Benzoyl-CoA:Anthranilate N-793 Hydroxycinnamoyl/Benzoyltransferase from Elicited Cell Cultures of Carnation, Dianthus caryophyllus L." Plant Molecular Biology 35 (6): 777–89. 794 Formatted: Portuguese (Brazil) 795 https://doi.org/10.1023/A:1005878622437. Formatted: Portuguese (Brazil) Yang, Qian, Hoat Xuan Trinh, Satoshi Imai, Atsushi Ishihara, Liqun Zhang, Hitoshi 796 Field Code Changed 797 Nakayashiki, Yukio Tosa, and Shigeyuki Mayama. 2004. "Analysis of the Involvement Formatted: Portuguese (Brazil) 798 of Hydroxyanthranilate Hydroxycinnamoyltransferase and Caffeoyl-CoA 3-O-Formatted: Portuguese (Brazil) 799 Methyltransferase in Phytoalexin Biosynthesis in Oat." Molecular Plant-Microbe Field Code Changed 800 Interactions: MPMI 17 (1): 81–89. https://doi.org/10.1094/MPMI.2004.17.1.81. Field Code Changed 801

Figure captions 802 803 804 Figure 1. Donor and acceptor substrates for HHHT. HHHT is capable of transferring a trans-805 hydroxycinnamic acid (here p-coumaric: R₁=H, R₂=OH; caffeic: R₁=OH, R₂=OH; ferulic 806 R₁=OCH₃, R₂=OH) from coenzyme A (CoA) to a hydroxyl group on mucic or saccharic acid to 807 form an ester. 808 Figure 2. Maximum likelihood phylogeny of clade Vb of BAHD acyltransferases. Sequences in 809 810 brown are from Phaseolus vulgaris, dark blue from Medicago truncatula, dark green from Trifolium pratense, light blue from Arabidopsis thaliana, green from Brachypodium distachion 811 and pink from Panicum hallii. 812 813 814 Figure 3. Protein sequence alignment showing the secondary structure of *Phaseoulus vulgaris* HHHT, as predicted by AlphaFold, and the sequence similarity with Trifolium pratense HMT 815 816 and HDT. Residues highlighted in red are conserved in all three proteins. Alignment was 817 performed by MUSCLE and visualized using ESPipt3. Residues in the active site interacting 818 with acyl donor substrates are marked with a circle, and those interacting with acyl acceptors are 819 marked with a star. 820 821 Figure 4. A. Expression profile of *Pvhhht* in pods, roots, leaves, stems, and seeds of *P. vulgaris* 822 cultivar 'Negro Jamapa' subjected to regular fertilization, or inoculated with effective nitrogen fixator strain Rhizobium tropici CIAT899, or with the ineffective Rhizobium Giardini 6917. 823 824 Values are mean FPKM obtained using RNA-seq. Data are from O'Rourke et al. 2014. B.

Expression profile of Pvhhht in leaves of P. vulgaris cultivar 'Sierra' after inoculation with the rust pathogen U. appendiculatus. Expression values were obtained using RNA-seq and are the log2 fold change at 12 hours versus 0 hours post-inoculation (12Ivs0I), 84 versus 0 hours post inoculation (84Ivs0I), and 84 versus 12 hours post-inoculation (84Ivs12I). Data are from Ayyappan et al., 2015. Figure 5. Abiotic stress-, copper-, hormone-, light-, pathogenic-, and nodulation-responsive ciselements present in the promoter sequence of Pvhhht (600 bp upstream of the transcriptional start). Directionality of the cis-elements relative to the gene is noted above the name and called "strand." The cis-elements labeled with asterisks (*) are palindromes and therefore do not have a direction. Figure 6. SDS-PAGE gel (10%) showing expression of his-tagged HHHT in E. coli and purification by immobilized metal affinity chromatography (IMAC). Lanes are uninduced culture, induced culture, soluble fraction, insoluble fraction, clarified soluble fraction applied to column (Pre-IMAC), unbound fraction, column wash, and eluate as indicated. All lanes were loaded with sample corresponding to $0.05\ \mathrm{OD}_{600\mathrm{nm}}$ of culture except eluate, which corresponds to 1.25 OD_{600nm} of culture. The arrow on the right marks the migration of the his-tagged protein. Figure 7. Kinetic curves showing rate (as ΔmA_{412nm}/min) versus substrate concentration. Data points are shown as means \pm standard error of the mean. R-squared values for the fit curves are all >0.94, with most (9 out of 12) > 0.97. Donor and acceptor substrates are as indicated.

825

826

827

828

829

830

831

832

833

834

835

836

837

838

839

840

841

842

843

844

845

846

847	$\Delta m A_{412nm}$ /min values were converted to katal as described in (Sullivan 2023) for calculation of
848	k_{cat} .
849	
850	Figure 8. PvHHHT structure predicted by alphafold. The two chloramphenicol acetyltransferase-
851	like domains are colored in blue and light orange.
852	
853	Figure 9. PvHHHT polar interactions with acyl acceptor ligands in the active site. A. Saccharic
854	acid. B. Mucic acid.
855	
856	Figure 10. PvHHHT polar interactions with acyl donor ligands in the active site. A. Caffeoyl. B.
857	<i>p</i> -Coumaroyl. C. Feruloyl.
858	
859	Figure 11. Relative specific activities of HHHT mutants compared to wild type. Activities were
860	measured with 100 μ M saccharic acid and 20 mM p -coumaric acid. One hundred percent
861	corresponds to 98.6 ketal/mg.
862	